EUROPEAN ORGANIZATION FOR NUCLEAR RESEARCH

Proposal to the ISOLDE and Neutron Time-of-Flight Committee

Microscopic insight by nuclear hyperfine methods on ferroic Perovskites

11th of January 2023

A.M.L. Lopes[1], J. H.-Schell[2,8], A. W. Carbonari[4], V.S. Amaral[3], J.P. Araujo[1], D. C. Lupascu[2], T. T. Dang[2], I. C. J. Yap[2], A. Burimova[4], J.G. Correia[5, 8], J.N. Gonçalves[3], A. L. Kholkin[3], A.A. Lourenço[3], R.P. Moreira[1], G.P. Oliveira[1], A. Cesário[1], P. A. Sousa[1], E.L. Silva[1], N. Lekshmi[1], G. A. Cabrera-Pasca[6], P. Rocha-Rodrigues[1], T. S. N. Sales[4], S.S.M. Santos[7], M.R. Silva[3], R. N. Saxena[4], A.A. Miranda Filho[4], N.P. Lima[4], H. M. Petrilli[6], L. V. C. Assali[6]

1 Institute of Physics for Advanced Materials, Nanotechnology and Photonics (IFIMUP), 4169 - 007 Porto
2 Institute for Materials Science and Center for Nanointegration Duisburg-Essen (CENIDE), University of Duisburg-Essen, 45141 Essen, Germany
3 Centre for Research in Ceramics and Composite Materials, CICECO, Aveiro University, 3810-193 Aveiro
4 Instituto de Pesquisas Energéticas e Nucleares - IPEN, São Paulo
5 Centro de Ciências e Tecnologias Nucleares (C2TN) Instituto Superior Técnico, Lisbon University, Lisbon
6 Instituto de Física da Universidade de São Paulo (IFUSP), São Paulo
7 Escola Politécnica da Universidade de São Paulo, São Paulo
8 European Organization for Nuclear Research (CERN), CH-1211 Geneva, Switzerland

Spokesperson(s): A.M.L. Lopes (armandina.lopes@fc.up.pt) and Juliana Schell (juliana.schell@cern.ch)
Local contact: J. G. Correia (guilherme.correia@cern.ch)

CERN-INTC-2023-027 / INTC-P-663
11/01/2023

Abstract

This proposal aims to study the crystal symmetry, electronic and magnetic properties, as well as their coupling effects in ferroic perovskites using nuclear hyperfine methods. The electrical field gradient and magnetic hyperfine field will be measured across phase transitions to study, at the local scale, their nature and elucidate the driving mechanisms behind the macroscopic properties. This project builds up on the previous experience using the perturbed angular correlations (PAC) technique on multiferroic materials to put forward a coordinated effort to study a set of intriguing ferroic materials. We will complement our local probe studies with conventional macroscopic methods, symmetry analysis and first-principles simulations (ab-initio methods based in Density Functional Theory). The use of appropriate PAC probe elements, such as the ^{111m}Cd/Cd and ^{204}Bi/Pb radioactive isotopes, specifically requires beams produced at ISOLDE.

Requested protons:28 shifts of protons on target, (split into at least 4 runs over 2 years)

Experimental Area: GLM area, ISOLDE hall and offline laboratories 508-r-008 and r-004

1. Motivation

The result of the global temperature rise is evident, and the nonstop societal and technological demands will accelerate the difficulties if no sustainable solutions became readily available. Fortunately, significant investments in the promotion and investigation of new promising materials, to be used as sources for green energy and ultra-low power consumption electronics are being made. In this respect, the high tunability of perovskite oxide systems and the control of their octahedra rotation and distortion, as well as the possibilities of their different dimensionalities allows to explore different functionalities. In the last years, advances in the synthesis, as well as, in first-principles calculation has given new insights into mechanisms and suggested new perovskite technological applications.

Nowadays, there are widely studied envisaging applications in spintronics, photovoltaics and photoelectrochemical cells, which harvest directly solar energy, or magnetization control by small electric pulses, via magnetoelectric effect for data processing and storage [1], [2]. In all cases, lattice distortions allows to adjust ferroic orders, and, in ferroelectric-photovoltaics these distortions can also effectively separate electron–hole pairs[3], [4].

The remarkable physical properties of perovskite ferroic materials may arise from a spontaneous symmetry breaking. Below this point, these materials display a non-centrosymmetric structure and while for proper-ferroelectrics the polarization is the primary order parameter, for improper-ferroelectrics, instead, the polarization is part of a more complex instability that can have different physical origins related to rotations or tilts of perovskite cages, magnetic or charge orderings [5], [6]. A trilinear coupling of non-polar lattice distortions can also induce ferroelectricity in even-layered systems [7].

Another fascinating property that has been found in some of these materials, is the capability of tuning their thermal expansion properties by chemical engineering. This is an important aspect since modern applications require functional materials to display not only good physical properties, but also controllable thermal expansion to enhance the reliability of devices.

To enlight the relations between crystallographic phases (e.g. with more/less oxygen octahedral cage rotation and/or distortion), materials composition, and the ferroic properties, a synergetic effort of solid-state chemists, physicists, and ab-initio computer-simulation experts is ongoing. Nevertheless, these materials properties are typically correlated to local landscapes, and they are not well described by long-range crystallographic/magnetic average models. In particular, the correct symmetries, how the lattice modes evolve within a symmetry and operating mechanisms need a different approach [8]9]. This symmetry related fine details can be monitored via precise hyperfine measurements as we recently reported [10-20]. Determining such atomic scale details, by measuring, for example, the electric field gradient (EFG) via Perturbed Angular Correlation, new strategies to create novel functional structures might eventually materialize.

The work here propose follows the collaborative research methodology of previous projects, such as IS647 and IS679, strengthened by the team experience in first-principles simulations with dedicated projects granted and running in the international PRACE supercomputing facility. Following previous PAC studies [5], [6], [10-21], obtained within IS647 and IS679 we now propose to study:

I) Controlling hybrid improper and proper ferroelectricity in naturally layered perovskites

II) Probing the switch from negative to positive thermal expansion perovskites related systems

III) Controlling improper ferroelectricity on doped rare-earth perovskites: $RMnO_3$ and RMn_2O_5 (R=Ho and Tb) cases

The specific motivations and proposed studies of each system are presented below.

Finally, the methods for sample production and for extended physical characterization (e.g polarization, magnetization, optoelectronic properties or Raman spectroscopy) are available at the proponent institutions. Neutron and synchrotron X-ray diffraction data, to be performed at Oak Ridge National Lab for which a new proposal has been accepted, will complement the local probe studies. Ab-initio Density functional theory (DFT) calculations, will be performed by the Porto University team supported by Dr. Helena Petrilli and Lucy Assali from the São Paulo University.
Finally, each topic constitutes the ground for students to develop their Phd-thesis, enabling them to master nuclear techniques, EFG simulations and/or theoretical aspects of multiferroic systems, according to their skills.

2. CASE STUDIES

I) Controlling hybrid improper and proper ferroelectricity in naturally layered perovskites

Hybrid improper ferroelectricity (HIF) discovered in naturally layered type perovskites such as the Ruddlesden-Popper (RP) and Dion Jacobson (DJ) phases, have contributed to significant progress in the past decade in the search for novel ferroelectric materials [22]. The polarization of RP and DJ compounds is determined by the combined effects of tilt/rotation modes. Using precise hyperfine measurements, we identified symmetry-related fine details around phase transition in conventional RP structured oxide $Ca_3Mn_2O_7$ (CMO) [10]. In contrast to conventional RP oxides, the origin of ferroelectricity is in debate for recently identified pseudo RP phases, such as $Li_2AB_2O_7$ (A=Ca, Sr and B=Nb, Ta), where HIF due to trilinear coupling compete with second order Jahn Teller (SOJT) induced polar mechanism [22]. In the pseudo RP phase, the Li^+ cations occupy the 4-coordinate tetrahedral sites rather than the 9-coordinate sites (Rock-salt layer) in conventional RP structure. Also, the Li_2O layer in pseudo RP $Li_2AB_2O_7$ is much thinner than the rock-salt layer (CaO) in the conventional RP CMO. Hence the out-of-plane interaction in $Li_2SrNb_2O_7$ is expected to be stronger than that in the CMO, which is responsible for the competing mechanisms for the ferroelectric phase transition and confering rich tunability for the ground state structure in pseudo RP oxides [23]. Hence in-depth understanding of structural features is required in these type of materials to shed new light on designing the phase transition and the polar instability namely by controlling the ionic radii of cations.

$Li_2ANb_2O_7$ (A=Sr, Ca)– Contradicting structural reports [Fig.1] on $Li_2SrNb_2O_7$ — (i) Room temperature polar *$A2_1am$* (36) phase, arising from HIF (octahedral tilting pattern: $a^-a^-c^+/a^-a^-c^+$), undergoes a structural phase transition to antiferroelectric *Pnma* (62) phase at 90 K (octahedral tilt pattern: $a^-a^-c^+/a^-a^-c^+$)[24]; and (ii) Room temperature non-polar *Cmcm* (63) phase (octahedral tilting pattern: $a^-a^-c^0/a^-a^-c^0$) changes to polar *$P2_1cn$* (33) phase at 217 K where the origin of ferroelectricity is the SOJT mechanism due to Nb^{5+} ion (d^0 cation) off-centring [25,26]. This also leads to uncertainty in confirming the compound's ground-state structure (polar vs antipolar). Recent first-principle calculations and dielectric studies opened-up the coexistence of HIF and SOJT mechanism for the ferroelectric phase transition on $Li_2Sr_{1-x}Ca_xNb_2O_7$ [23]. Hence the disparity in the ground state structure and origin of polarization in $Li_2ANb_2O_7$ highlights the challenge of unambiguously determining the subtle structural distortions, a scenario worth exploring by local, nanoscopic probing via PAC.

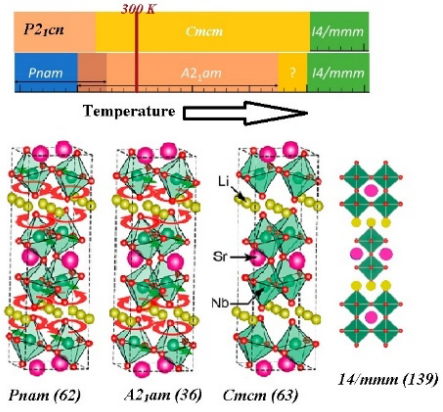

Fig.1: $Li_2SrNb_2O_7$ conflicting structural paths

$MnSrB_2O_7$ (B=Nb,Ta) –$Li_2SrB_2O_7$ is also identified as a cation-exchange host (for M^{2+} cations), thereby stabilizing the HIF mechanism and allowing the preparation of novel magneto-electric materials, for example, $MnSrTa_2O_7$ [27]. At room temperature, $MnSrTa_2O_7$ exhibits polar *$A2_1am$* (S.G.36) phase due to HIF, which on cooling below 43 K adopts a canted antiferromagnetic state and shows magneto-electric coupling below 38 K. To date, the only magneto-electric multiferroic materials identified based on the HIF mechanism are CMO and $[Ca_{0.69}Sr_{0.46}Tb_{1.85}Fe_2O_7]0.85[Ca_3Ti_2O_7]0.15$, which makes $MnSrB_2O_7$ an exciting candidate for local probe studies.

$RbA_2Nb_3O_{10}$ (A=Ca, Cd)– DJ phases have many conflicting structural reports. According to Benedek [8], several double-layered DJ phases that have been previously identified experimentally as non-polar phases might, in fact, be polar, which prompted a revisit on these DJ oxides. The prediction by Benedek was successfully confirmed, and polar ground structure was identified on double-layered DJ by Tong *et al.* [29,30] in a recent study using a combination of theory and neutron diffraction experiments. This led us to revisit the triple layer DJ oxide and probe the structural studies on $RbCa_2Nb_3O_{10}$, previously identified as a non-polar tetragonal *P4/mmm* [31]. Since the mechanism of HIF is not applicable in triple layer DJ oxides, however, the presence of Nb^{5+} ion (d^0) off-centring can induce SOJT mechanism of polarization in $RbCa_2Nb_3O_{10}$, a powerful context in terms of local probe studies. In addition, very recently, Atri *et al.* [32] identified $RbCd_2Nb_3O_{10}$ with noncentrosymmetric orthorhombic (*Ima2*) structure due to the coupled interaction of SOJT (Nb^{5+}-d^{10}) and enhanced lattice covalency (Cd^{2+}-d^{10}), projecting it as another excellent platform for local probe studies in three layered DJ materials.

During our last beam time, we measured the 300 K PAC spectrum of $Li_2SrNb_2O_7$ [Fig. 2] however, to resolve the conflicting ground state symmetry and structural transition pathways and unveil how the order parameters evolve within the different polar natures upon Sr/Ca doping ***(HIF+SOJT)*** and Li/Mn ***(HIF and magneto-electric)*** substitution, it is necessary to invest in the collection and analysis of PAC data for $Li_2SrNb_2O_7$, $Li_2Sr_{1-x}Ca_xNb_2O_7$ and $MnSrNb_2O_7$**.** Also, we are interested in investigating the possibility of polar ground-state structure in $RbCa_2Nb_3O_{10}$ ***(SOJT)*** and elucidating the cooperative influence of d^0 and d^{10} cations in stabilizing the non-polar structure of $RbCd_2Nb_3O_{10}$ ***(SOJT+enhanced covalency)***. Hence, we propose to study PAC experiments on these materials to investigate local properties at the cation sites.

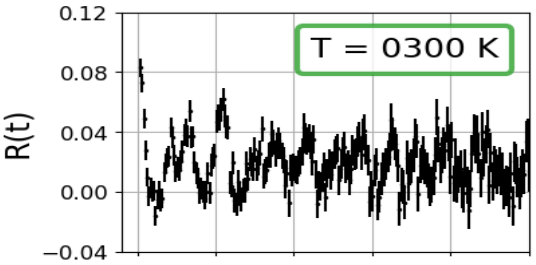

Fig.2: PAC spectra obtained for $Li_2SrNb_2O_7$ during our last

II) Probing the switch from negative to positive thermal expansion perovskites related systems

Another approach for the search for novel ferroelectric materials focuses on the synthesis of partially A site substituted n=1 $A'O(ABO_3)_n$ RP systems [33,34]. However, another interesting functional property that has been found in some of these materials, is the capability of tuning their thermal expansion properties by chemical engineering, including the ability to switch from positive to uniaxial or biaxial negative thermal expansion (NTE) by performing small ionic substitutions [35-36].

Several intrinsic mechanisms are known to be able to induce NTE, these can be based on structural mechanisms, such as NTE driven by transverse vibrational modes, observed in frameworks of corner-sharing metal-anion tetrahedra or octahedra units [38,39], or, for instance, based on transitions between different electronic or magnetic states that are strongly coupled to the crystal lattice [40,41]. According to the Symmetry Trapping mechanism, the presence of low energy phonon modes corresponding to transverse vibrations of the BO_6 octahedral units, was proposed to drive the NTE in the RP manganite systems [42]. Later, the condensation of BO_6 octahedral distortion modes in the layered structure of the RP systems, were shown to be essential to enhance the elastic compliance

anisotropy required for the development of NTE on these systems [43, 44]. Notably, among the distinct dimensionalities of the Ruddlesden-Popper (RP) family, the n=1 oxide systems (A_2BO_4) are expected to present the highest uniaxial NTE. At the atomic scale, by combining PAC measurements with temperature-dependent Neutron Diffraction studies on the Ca_2MnO_4 system, we were able to follow the atomic corkscrew mechanism governing the enhancement of the contraction of crystal lattice, along the stacking-axis, across the structural transition from the distorted $I4_1/acd$ structure to the aristotype $I4/mmm$ phase [16]. Recent reports based on high-resolution X-ray diffraction measurements performed on the $Ca_{2x}Sr_xMn_{1-y}Ti_yO_4$ series have shown that the magnitude of uniaxial NTE can increase as the weight of manganese to titanium substitution increases, down to the limit where the structural phase $I41/acd$ characterized by NTE is no longer stable, with the observation of a secondary structural phase of unknown symmetry (y>0.65) [36]. We have already performed some room temperature PAC measurements on the $Ca_2Mn_{1-y}Ti_yO_4$ series, as represented by the perturbation function, R(t), illustrated in Fig. 3. In future experiments, we expect to study the temperature dependency EFG strength, to see if we can follow the change of frequency of the low energy phonon modes that drive the NTE according to the Symmetry Trapping model [13]. Furthermore, for high values of manganese by titanium substitution (y>0.65) we will study the structural transition followed by the material while decreasing temperature below 200 K, particularly, across the temperature window where the switch from uniaxial NTE to PTE was reported [36].

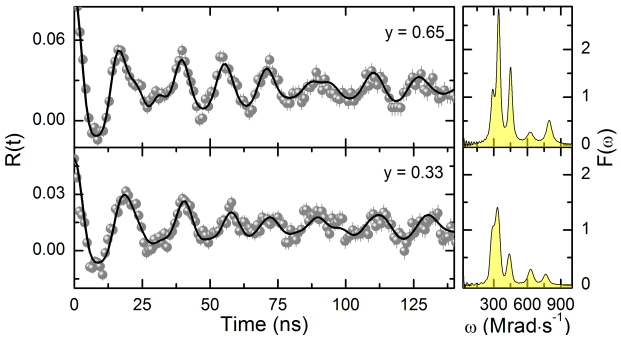

Fig. 3 - R(t), measured at room temperature after ^{111m}Cd beam implantation on bulk polycrystalline $Ca_2Mn_{1-y}Ti_yO_4$, (y = 0.65, 0.33) samples.

III) Controlling improper ferroelectricity on doped rare-earth perovskites: $RMnO_3$ and RMn_2O_5 (R=Ho and Tb) cases

The perovskite family $RMnO_3$ and RMn_2O_5 (where R is a rare-earth element, e.g., Ho, Tb, La, etc.) present a vast number of physical properties such as ferroelectricity, and colossal magnetoresistance. Among these compounds, the rare-earth manganites, also point to applications in fundamental physics perspectives since spin-charge–orbital coupled systems in transition-metal oxides, i.e., a strong coupling between ferroelectricity and magnetism, offer a wide field of investigation [45]. Several studies of materials like perovskites $RMnO_3$ and RMn_2O_5 have shown magnetocaloric effects associated with commensurate-incommensurate magnetic transitions [46]. Therefore perovskite-like structures have potential applications in spintronics, data storage, and sensors [47]. Among the techniques that characterize these structures, the Perturbed Angular Correlation (PAC) has great potential to produce valuable information about the interaction mechanisms in multiferroic oxides due to their local character and action on a subnanoscopic scale, those based on hyperfine interactions. Here, we aim to investigate the temperature dependence of hyperfine interactions in pure, Cd/ La doped RMnO3 and RMn2O5 (R = Tb, Ho) oxides using the PAC technique. Doping alters

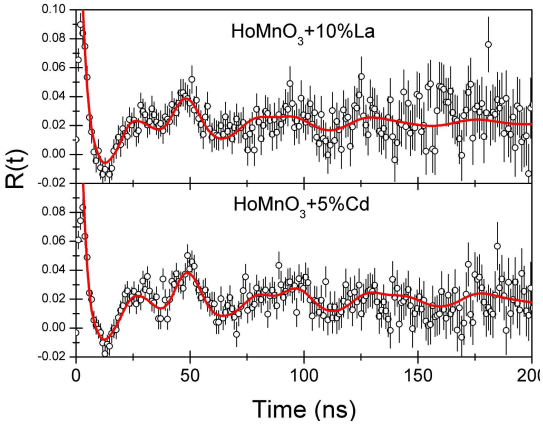

*F*ig. 4 - Perturbation functions, R(t), measured at room temperature after ^{111m}Cd beam implantation for $HoMnO_3$ doped with 10% of La and 5% of Cd.

the Mn3+/Mn4+ ratio, which is primarily responsible fo r the magnetic interaction [53]. As shown in the TDPAC spectra, that was measured at room temperature with ^{111m}Cd for $HoMnO_3$ doped with 10% of La and 5% of Cd, the doping with La shows a smaller distortion (eta = 0.22) than with Cd (eta =0.29) even at a higher concentration.

HoMnO3, HoMn2O5 and Tb-related systems will be studied across their rich phase diagrams, shown below in fig 5 and 6 [48], [50] [51] and the effect of doping with La and Cd will be evaluated. We propose to study these perovskites using ^{111m}Cd to probe the R site of the perovskites. Complementary measurements using ^{140}La(^{140}Ce) probe, very sensitive to magnetic hyperfine interactions, will be performed IPEN, São Paulo.

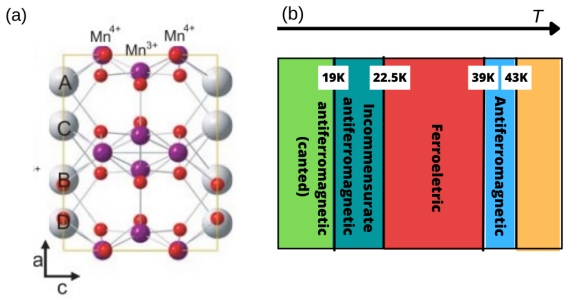

Fig. 5 - (a) Crystal structure of the perovskite $HoMn_2O_5$ [50]. (b) Sequence of some phase transitions in $HoMn_2O_5$.

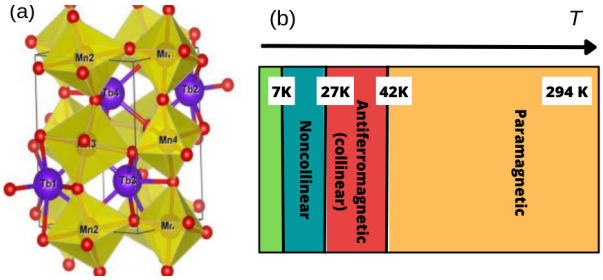

Fig. 6 - (a) Crystal structure of the perovskite $TbMn_2O_5$ [52]. (b) Sequence of some phase transitions in $TbMn_2O_5$.

Summary of requested protons:

The work plan assigns one specific case study to each team of experts of the collaboration. The complementarity of the systems allows, through collaborative work and efficient use of equipment and resources, to obtain an integrated view of the role of local distortions upon tuning ferroic properties.

ISOLDE Beam	Intensity (ion/μC of p-beam)	Target	Ion source	SHIFTS per year	Systems
^{111m}Cd (48 m)	1.10^8	Molten Sn	Vadis MK5	12 (2 per system)	Li2ANb2O7 (A=Sr, Ca) MnSrB2O7 (B=Nb,Ta) RbA2Nb3O10 (A=Ca, Cd) Ca2Mn1–yTiyO4 RAMn2O5 RAMnO3

^{111}In (2.8d)*	1.10^6	UC_2	Surface	1	Li2ANb2O7 (A=Sr, Ca) RbA2Nb3O10 (A=Ca, Cd)
^{204}Bi (11.2h) ^{204m}Pb (67m)	$1 .10^7$ $5 .10^7$	UC_2	RILIS	1	Li2ANb2O7 (A=Sr, Ca) RbA2Nb3O10 (A=Ca, Cd)

^{111m}Cd/Cd – is the main probe isotope required to achieve our aims, considering that it has been successfully tested in most compounds under study. Willing to explore the B site(s) we consider experimental campaigns using ^{181}Hf/^{181}Ta($t_{1/2}$ =45d) with the help of the ISKP Bonn implanter. ^{204}Bi/Pb:. Bi isotope is also a suitable probe as Bi usually replaces the A PK site. Experiments using ^{204}Bi/Pb will profit from the use of digital setups with LaBr3 scintillators that separate γ_1 (912 keV) of ^{204m}Pb (~14%) from γ_1 (984 keV) (~59%) after ^{204}Bi decay [54].
* when available without disturbing main user. Yields can be higher if RILIS available, preferentially near shutdowns due to the long halflife.

References:

[1] R. Ramesh and N. A. Spaldin, "Multiferroics: progress and prospects in thin films," Nat. Mater., vol. 6, no. 1, pp. 21–29, 2007.

[2] M. Bibes and A. Barthélémy, "Multiferroics: Towards a magnetoelectric memory," Nat. Mater., vol. 7, no. 6, pp. 425–426, 2008.

[3] H. Wang, G. Gou, and J. Li, "Ruddlesden-Popper perovskite sulfides A3B2S7: A new family of ferroelectric photovoltaic materials for the visible spectrum," Nano Energy, vol. 22, pp. 507–513, 2016.

[4] I. E. Castelli, T. Olsen, and Y. Chen, "Towards photoferroic materials by design: recent progress and perspectives," J. Phys. Energy, vol. 2, no. 1, p. 011001, 2019.

[5] A. M. L. Lopes, J. P. Araújo, V. S. Amaral, J. G. Correia, Y. Tomioka, and Y. Tokura, "New phase transition in the $Pr_{1-x}Ca_xMnO_3$ system: Evidence for electrical polarization in charge ordered manganites," Phys. Rev. Lett., vol. 100, no. 15, p. 155702, 2008.

[6] G. N. P. Oliveira, R. C. Teixeira, R. P. Moreira, J. G. Correia, J. P. Araújo, and A. M. L. Lopes, "Local inhomogeneous state in multiferroic $SmCrO_3$," Sci. Rep., vol. 10, no. 1, pp. 1–12, 2020.

[7] N. A. Benedek and C. J. Fennie, "Hybrid improper ferroelectricity: A mechanism for controllable polarization-magnetization coupling," Phys. Rev. Lett., vol. 106, no. 10, p. 107204, 2011.

[8] B. H. Chen, T. L. Sun, X. Q. Liu, X. L. Zhu, H. Tian, and X. M. Chen, "Enhanced hybrid improper ferroelectricity in $Sr_{3-x}Ba_xSn_2O_7$ ceramics with a Ruddlesden-Popper (R-P) structure," Appl. Phys. Lett., vol. 116, no. 4, p. 042903, 2020.

[9] S. Yoshida et al., "Hybrid Improper Ferroelectricity in $(Sr,Ca)_3Sn_2O_7$ and Beyond: Universal Relationship between Ferroelectric Transition Temperature and Tolerance Factor in n = 2 Ruddlesden-Popper Phases," J. Am. Chem. Soc., vol. 140, no. 46, pp. 15690–15700, 2018.

[10] P. Rocha-Rodrigues et al., "$Ca_3Mn_2O_7$ structural path unraveled by atomic-scale properties:

A combined experimental and ab initio study," Phys. Rev. B, vol. 101, no. 6, p. 64103, 2020.

[11] G. N. P. Oliveira et al., "Dynamic off-centering of Cr^{3+} ions and short-range magneto-electric clusters in $CdCr_2S_4$," Phys. Rev. B - Condens. Matter Mater. Phys., vol. 86, no. 22, p. 224418, 2012.

[12] J. N. Gonçalves et al., "Ab initio study of the relation between electric polarization and electric field gradients in ferroelectrics," Phys. Rev. B - Condens. Matter Mater. Phys., vol. 86, no. 3, p. 035145, 2012.

[13] A. M. L. Lopes et al., "Local distortions in multiferroic $AgCrO_2$ triangular spin lattice," Phys. Rev. B - Condens. Matter Mater. Phys., vol. 84, no. 1, p. 014434, 2011.

[14] G. N. P. Oliveira et al., "Local Probing ErCrO3", Crystals, 13(1), 54, 2023.

[15] S. S. M. Santos et al., "Spontaneous electric polarization and electric field gradient in hybrid improper ferroelectrics: insights and correlations", J. Mater. Chem. C, 2021,9, 7005-7013, 2021.

[16] P. Rocha-Rodrigues et al., "Ca_2MnO_4 Structural Path: Following the Negative Thermal Expansion at the Local Scale", Physical Review B 102 (10):104115, 2020.

[17] J. Schell, H. Hofsäss, and D. C. Lupascu, "Using radioactive beams to unravel local phenomena in ferroic and multiferroic materials," Nucl. Instruments Methods Phys. Res. Sect. B Beam Interact. with Mater. Atoms, vol. 463, pp. 134–137, Jan. 2020.

[18] B. Bosch-Santos, N. M. Nascimento, M. Saiki, E. L. Correa, T. S. N. Sales, L. F. D. Pereira, G. A. Cabrera-Pasca, R. N. Saxena, J. Schell, and A. W. Carbonari, "Magnetic field at Ce impurities in La sites of $La_{0.5}Ba_{0.5}MnO_3$ double perovskites", AIP Advances **9**, 035245, 2019.

[19] G. Marschick et al., "Multiferroic bismuth ferrite: Perturbed angular correlation studies on its ferroic α β phase transition Physical Review B 102, 224110, 2020.

[20] J. Schell et al., "Strong magnetoelectric coupling at an atomic nonmagnetic electromagnetic probe in bismuth ferrite", Physical Review B 105, 094102, 2022.

[21] T. T. Dang et al., "Temperature dependence of the local electromagnetic field at the Fe site in multiferroic bismuth ferrite", Physical Review B 106, 054416, 2022.

[22] N. A. Benedek et al., "Hybrid Improper Ferroelectricity: A Theoretical, Computational, and Synthetic Perspective," Annu. Rev. Mater. Res. 52:331–55, 2022.

[23] Y. Mochizuki et al., "Coexisting Mechanisms for the Ferroelectric Phase Transition in Li2SrNb2O7," Chem. Mater., 33, 1257 1264, 2021.

[24] R. Uppuluri et al., "Competing Polar and Antipolar Structures in the Ruddlesden Popper Layered Perovskite Li2SrNb2O7," Chem. Mater. 31, 4418–25, 2019.

[25] T. Nagai et al., "Phase Transition from Weak Ferroelectricity to Incipient Ferroelectricity in Li2Sr(Nb1–xTax)2O7," Chem. Mater. 32, 744–50, 2020.

[26] T. Nagai et al., "Weak Ferroelectricity in n = 2 Pseudo Ruddlesden–Popper-Type Niobate Li2SrNb2O7," Chem. Mater. 31, 6257–61, 2019.

[27] T. Zhu et al., "Directed synthesis of a hybrid improper magneto-electric multiferroic material," NATURE COMMUNICATIONS 12, 4945, 2021.

[28] N. A. Benedek, "Origin of Ferroelectricity in a Family of Polar Oxides: The Dion—Jacobson Phases," Inorg. Chem. 53, 3769, 2014.

[29] T. Zhu et al., "Theory and Neutrons Combine To Reveal a Family of Layered Perovskites without Inversion Symmetry," Chem. Mater. 29, 9489, 2017.

[30] T. Zhu et al., "Complex Structural Phase Transitions of the Hybrid Improper Polar Dion–

Jacobson Oxides RbNdM2O7 and CsNdM2O7 (M = Nb, Ta),” Chem. Mater. 32, 4340, 2020.

[31] Z-H. Liang et al., RbCa2Nb3O10 from X-ray powder data, Acta Cryst., E65, i44, 2009.

[32] S. Atri et al., "Synergistic Influence of d0 (Nb^{5+}) and d10 (Cd^{2+}) Cations in Stabilizing Noncentrosymmetric Dion Jacobson Layered Perovskites, A′Cd2Nb3O10 (A′ = Rb, Cs)," Inorg.Chem., 59, 12, 8044–8053, 2020.

[33] A. T. Mulder et al., “Turning ABO_3 antiferroelectrics into ferroelectrics: Design rules for practical rotation-driven ferroelectricity in double perovskites and $A_3B_2O_7$ Ruddlesden-popper compounds. Advanced Functional Materials”, 23(38):4810–4820, 2013.

[34] A. S. Gupta et al., “Competing structural instabilities in the ruddlesden-popper derivatives $HRTiO_4$ (R = rare earths): Oxygen octahedral rotations inducing noncentrosymmetricity and layer sliding retaining centrosymmetricity”, Chemistry of Materials, 29:656–665, 1, 2017.

[35] M. S. Senn et al., “Symmetry Switching of Negative Thermal Expansion by Chemical Control”, Journal of the American Chemical Society, 138(17):5479–5482, may 2016.

[36] C. Ablitt et al., “Tolerance Factor Control of Uniaxial Negative Thermal Expansion in a Layered Perovskite. Chemistry of Materials, 32(1):605–610, 2020.

[37] S. Yoshida, et al., “Interplay between oxygen octahedral rotation and deformation in the acentric $ARTiO_4$ series toward negative thermal expansion”, Chemistry of Materials, 34:6492–6504, 7, 2022.

[38] T. A. Mary, J. S. O. Evans, T. Vogt, and A. W. Sleight. “Negative Thermal Expansion from 0.3 to 1050 Kelvin in ZrW2O8”, Science, 272(5258):90–92, 1996.

[39] J. Chen et al., “Tunable thermal expansion in framework materials through redox intercalation”, Nature Communications, 8(1):14441, 2017.

[40] J. Paul Attfield, “Mechanisms and Materials for NTE”, Frontiers in Chemistry, 6, 2018.

[41] K. Takenaka, “ Progress of Research in Negative Thermal Expansion Materials: Paradigm Shift in the Control of Thermal Expansion”. Frontiers in Chemistry, 6, jul 2018.

[42] M. S. Senn, A. Bombardi, C. A. Murray, C. Vecchini, A. Scherillo, X. Luo, and S. W. Cheong. “Negative thermal expansion in hybrid improper ferroelectric Ruddlesden-popper Perovskites by symmetry trapping”. Physical Review Letters, 114(3):23–27, 2015.

[43] C. Ablitt, S. Craddock, M. S. Senn, A. A. Mostofi, and N. C. Bristowe. “The origin of uniaxial negative thermal expansion in layered perovskites”, npj Computational Materials”, 3 (1). 44, 2017.

[44] W.-T. Chen et al., “Negative thermal expansion in high pressure layered perovskite Ca2GeO4”, Chemical Communications, 55(20):2984–2987, 2019.

[45] V. Hreb, I. Lutsyuk, V. Kochubei, and L. Vasylechko, “New Mixed Manganites-chromites $RMn_{1-x}Cr_xO_3$ and Manganites-gallates $RMn_{1-x}Ga_xO_3$” 2020 IEEE 10th International Conference Nanomaterials: Applications \& Properties (NAP), pp. 1-6, 2020.

[46] Endichi, A., Bouhani, H., Zaari, H. et al. Electronic and magnetic properties of the multiferroic TbMn2O5. Appl. Phys. A 126, 410, 2020.

[47] H.W. Brinks, H. Fjellvåg, A. Kjekshus, Synthesis of Metastable Perovskite-type $YMnO_3$ and $HoMnO_3$, Journal of Solid State Chemistry, vol. 129, pp. 334-340 , 1997.

[48] K. Shimamoto et al. Multiferroic properties of uniaxially compressed orthorhombic HoMnO3 thin films. Applied Physics Letters, v. 108, n. 11, p. 112904, 2016.

[49] Fedorova, Natalya & Ederer, Claude & Spaldin, Nicola & Scaramucci, Andrea, “Biquadratic

and ring exchange interactions in orthorhombic perovskite manganites", Physical Review B. 91. 10.1103, 2014.

[50] I. Radulov, et al. "Colossal magnetostriction effect in HoMn2O5" Eur. Phys. J. B 52, 361–364, 2006.

[51] Kassimi, Fatima Zahrae, et al. "A theoretical study of the electronic, magnetic and magnetocaloric properties of the $TbMnO_3$ multiferroic." Journal of Magnetism and Magnetic Materials 543, 168397, 2022.

[52] Endichi, A., Bouhani, H., Zaari, H. et al. Electronic and magnetic properties of the multiferroic $TbMn_2O_5$. Appl. Phys. A 126, 410, 2020.

[53] I. A. Zobkalo, S. V. Gavrilov, V. A. Sanina, E. I. Golovenchits, Temperature hysteresis of magnetic phase transitions in $Tb_{1-x}Ce_xMn_2O_5$ (x = 0, 0.20, 0.25). Phys. Solid State 56, 51, 2014.

[54] M. Nagl, U. Vetter, M. Uhrmacher, and H. Hofsäss, "A new all-digital time differential γ-γ Angular correlation spectrometer," *Rev. Sci. Instrum.*, vol. 81, no. 7, p. 073501, Jul. 2010, doi: 10.1063/1.3455186.

Appendix

DESCRIPTION OF THE PROPOSED EXPERIMENT

Please describe here below the main parts of your experimental set-up:

Part of the experiment	Design and manufacturing
Standard, existing equipments, inside the solid-state labs of building 508: r-002 (chemical lab), r-004 (annealing furnaces room) and r-008 (PAC spectrometer's room)	☒ To be used without any modification ☐ To be modified
SSP-chamber @ GLM Standard general purpose collection chamber mounted at GLM. https://edms.cern.ch/document/1693386/1	☒ To be used without any modification ☐ To be modified
ISOLDE-170 Fume Hood @ GLM-GHM area Fume Hood to handle freshly implanted sample and sample holders	☒ To be used without any modification ☐ To be modified
[insert lines if needed]	

HAZARDS GENERATED BY THE EXPERIMENT

Additional hazard from flexible or transported equipment to the CERN site:

Domain	Hazards/Hazardous Activities		Description
Mechanical Safety	Pressure	☒	bottles of compressed gases for annealing such as Argon and Nitrogen may be required
	Vacuum	☒	10-6 mbar at SSP chamber @ GLM during collections
	Machine tools	☐	
	Mechanical energy (moving parts)	☐	

	Hot/Cold surfaces	☒	Quartz tube used for annealing at 508/R-004
Cryogenic Safety	Cryogenic fluid	☒	Liquid nitrogen, 1 Bar, few litres used during the PAC measurements on appropriate dewars
Electrical Safety	Electrical equipment and installations	☒	[220] [V], [16] [A]
	High Voltage equipment (PAC detectors)	☒	[<2900] [V]
Chemical Safety	CMR (carcinogens, mutagens and toxic to reproduction)	☐	[fluid], [quantity]
	Toxic/Irritant	☐	[fluid], [quantity]
	Corrosive	☐	[fluid], [quantity]
	Oxidizing	☐	[fluid], [quantity]
	Flammable/Potentially explosive atmospheres	☐	[fluid], [quantity]
	Dangerous for the environment	☐	[fluid], [quantity]
Non-ionizing radiation Safety	Laser	☐	[laser], [class]
	UV light	☐	
	Magnetic field	☐	[magnetic field] [T]
Workplace	Excessive noise	☐	
	Working outside normal working hours	☒	Yes, if beam time is scheduled 24 h per day
	Working at height (climbing platforms, etc.)	☐	
	Outdoor activities	☐	
Fire Safety	Ignition sources	☐	
	Combustible Materials	☐	
	Hot Work (e.g. welding, grinding)	☐	
Other hazards	Ionizing radiation	☒	Measurements will be performed with ^{111m}Cd Pb or or ^{111}In therefore a zone properly classified should be available for the equipment during the experiments.